Interface Dynamics for Bacterial Colony Formation

So Kitsunezaki *

Department of Physics, Graduate School of Sciences,
Kyoto University, Kyoto 606, Japan

(Received July 31, 1999)

We propose a differential-equation model with a nonlinear diffusion term for explaining pattern formation of bacterial colonies, and carry out its numerical simulations. Our model is reduced to an interface dynamics by means of a systematic perturbation method. This is similar to a model system for viscous fingering except that the field around an interface obeys a diffusion equation and that surface tension does not work on the interface. How the difference in morphology results depending on the condition is explained qualitatively.

KEYWORDS: bacterial colony, Bacillus subtilis, pattern formation, interface dynamics, nonlinear diffusion, Fisher's equation, random lattice

§1. Introduction

Bacteria are relatively simple organisms and their behavior is restricted severely by the environment. Under bad conditions, they often exhibit patterns similar to those in many physical systems such as fingering patterns.

In recent years, pattern formation of bacterial colonies for some kinds of species has been studied enthusiastically[1-3]. In particular, a complete phase diagram has been obtained for the colonies of *Bacillus subtilis*, where the important control parameters are the concentration of agar C_a and that of the initial nutrient n_0 in an agar culture medium. The resulting phase diagram includes some interesting regimes such as diffusion limited aggregation(DLA), dense branching morphology(DBM), Eden-like and ring patterns[4-6]. In this paper, we concentrate on this particular species of bacteria.

A number of models have been proposed so far to explain these experiments and succeeded in reproducing some of the patterns observed[6-10]. Still, they are unable to provide a simple description of pattern formation so that the results may be compared with similar phenomena in physical systems.

In §2, we propose a differential-equation model with a nonlinear diffusion term. The results of its numerical simulations are consistent with experiments, which will be discussed in §3. We reduce our model to an interface dynamics in §4, and from this viewpoint, pattern formation of bacterial colonies is revisited in §5. Some conclusions are given in §6.

§2. Modeling

Bacteria eat nutrient, move around rather randomly and increase in number by splitting on the surface of an agar culture medium. In poor-nutrient condition, they suspend these actions and transform to a special form for dormancy. For simplicity, we discretize the state of bacteria into two, i.e., active and inactive states. The bacterial density is represented as a sum of the densities of active and inactive bacteria, each represented by $b(\mathbf{x},t)$ and $a(\mathbf{x},t)$, respectively. The same idea was also used in other models[8,10]. We moreover assume that the movement of the active bacteria is influenced by neither the nutrient concentration $n(\mathbf{x},t)$ nor the inactive bacterial density $a(\mathbf{x},t)$. Because in experiments the bacteria hardly recover from the dormant form, we need to consider only the change from the active state to the inactive one. Therefore, the bacterial growth will qualitatively follow the equations

$$\partial_t b = \nabla[D(b)\nabla b] + g(n,b) - h(n,b) \tag{2.1a}$$

and

$$\partial_t a = h(n,b), \tag{2.1b}$$

where $D(b)$ is a diffusion coefficient of the active bacteria and g and h are the rates of increase and dormancy, respectively.

The nutrient is prepared uniformly in the agar before the inoculation of the bacteria with the initial nutrient concentration $n(\mathbf{x},0) = n_0$. Because the agar plates used in the aforementioned experiments are sufficiently thin, the nutrient concentration $n(\mathbf{x},t)$ practically obeys a two-dimensional diffusion equation with a consumption term

$$\partial_t n = D_n \triangle n - f(n,b), \tag{2.2}$$

where D_n is the diffusion constant of the nutrient and f is the consumption rate.

Equations (2.1) and (2.2) give a closed set of equations for the nutrient concentration $n(\mathbf{x},t)$ and the active bacterial density $b(\mathbf{x},t)$, although what we observe in real situation is the total bacterial density $b(\mathbf{x},t) + a(\mathbf{x},t)$.

To determine the functions f, g and h, we impose the following conditions which seem natural:

i) For the rate of consumption, $f(0,b) = f(n,0) = 0$, and $f(n,b)$ increases with n and b.

* E-mail: kitsune@ton.scphys.kyoto-u.ac.jp

ii) For the rate of increase, $g(0,b) = g(n,0) = 0$, and $g(n,b)$ increases with n and b.
iii) For the rate of dormancy, $h(n,0) = 0$, and $h(n,b)$ increases with b.

For simplicity, we consider only the linear functions to satisfy these conditions, i.e., $f, g \propto bn$ and $h \propto b$.

The diffusion coefficient $D(b)$ characterizes the movement of bacteria. In experiments for higher agar concentration C_a, the agar becomes stiffer so that the bacteria can hardly move unless they swarm. Therefore, we expect $D(0) = 0$ when C_a is large. This is also supported by the observation through microscope for the real interface of the bacterial colonies. The bacterial density decays gradually to zero at the interface under the small-C_a condition, as is expected in the case of finite diffusion $D(0) \neq 0$. Under large-C_a condition, on the contrary, the interface forms a very sharp wall with the width only of a few times as thick as the bacterial size. In order to investigate how the difference between normal and nonlinear diffusion reflects on the pattern formation, we choose the diffusion coefficient as $D(b) \propto b^k$, where $k = 0$ corresponds to the normal diffusion.

After suitable scaling, we obtain equations with three non-negative parameters D, μ and k in the forms

$$\partial_t n = \triangle n - nb, \tag{2.3a}$$

$$\partial_t b = D\triangle(b^{k+1}) + (n-\mu)b \tag{2.3b}$$

and

$$\partial_t a = \mu b. \tag{2.3c}$$

The initial conditions are set $n(x,y,t) = 1$ and $b(x,y,t) = b_0(x,y)$, the latter depending on how the bacteria are incubated. No-flux conditions are imposed at the boundary of the agar culture medium, or we may use the boundary conditions $n(x,y,t) \to 1$ and $b(x,y,t) \to 0$ as $|\mathbf{x}| \to \infty$ instead. In the subsequent sections, we examine the behavior of the solutions of this model.

§3. Simulations

In this section, we investigate the model proposed above by numerical simulations. This system has sensitivity to anisotropy which is inherent in fingering patterns. In order to remove artificial anisotropy produced by a regular-lattice model, we use a random lattice[11, 12] composed of Voronoi cells generated by random points (see Fig.1).

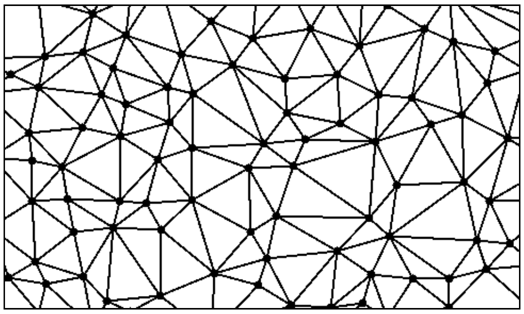

Fig. 1. Random lattice

We let the length l between neighboring points have a lower limit l_0 so that we may use the Euler method. Without introducing any artificial noise in the simulations, randomness comes naturally from the distributions of the length l and the volume v of the cells such as shown in Fig.2.

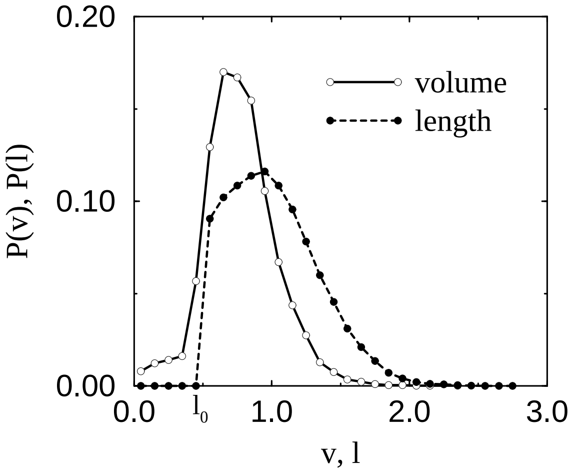

Fig. 2. The distributions of the length l between neighboring points and the volume v of the cells.

The simulations were carried out for $k = 0, 1, 2$ and 3 on the lattice with 10000 sites whose horizontal and vertical extensions are $(L_x, L_y) = (200, 40)$. We imposed periodic conditions on the horizontal boundaries, no-flux conditions on the left vertical one and fixed conditions $b(\mathbf{x},t) = 0$ and $n(\mathbf{x},t) = 1$ on the right vertical one. The initial conditions assumed are $n(\mathbf{x},0) = 1$, $a(\mathbf{x},0) = 0$ and $b(\mathbf{x},0) = 0.01\Theta(5-x)$ where $\Theta(x)$ is the Heaviside step function.

The results of the simulations are summarized as follows.

- When k vanishes, the interface of a growing colony forms a stable straight interface regardless of the values of the other parameters μ and D. The interface propagates with a constant speed which increases with D and decreases with μ.
- When $k > 1$, the straight interface loses stability either as D decreases or as μ increases, which is shown in Fig.3. For small D and vanishing μ, the interface develops some dented cusps, although they do not develop into grooves. In contrast, fingering patterns appear for non-vanishing μ and they become fractal-like patterns with increasing μ and decreasing D. At the same time, they grow slowly and the total bacterial density increases.

These results are consistent with the experiments[4-6] introduced in §1. The initial nutrient concentration n_0 before the scaling is represented by $1/\mu$ except for a mul-

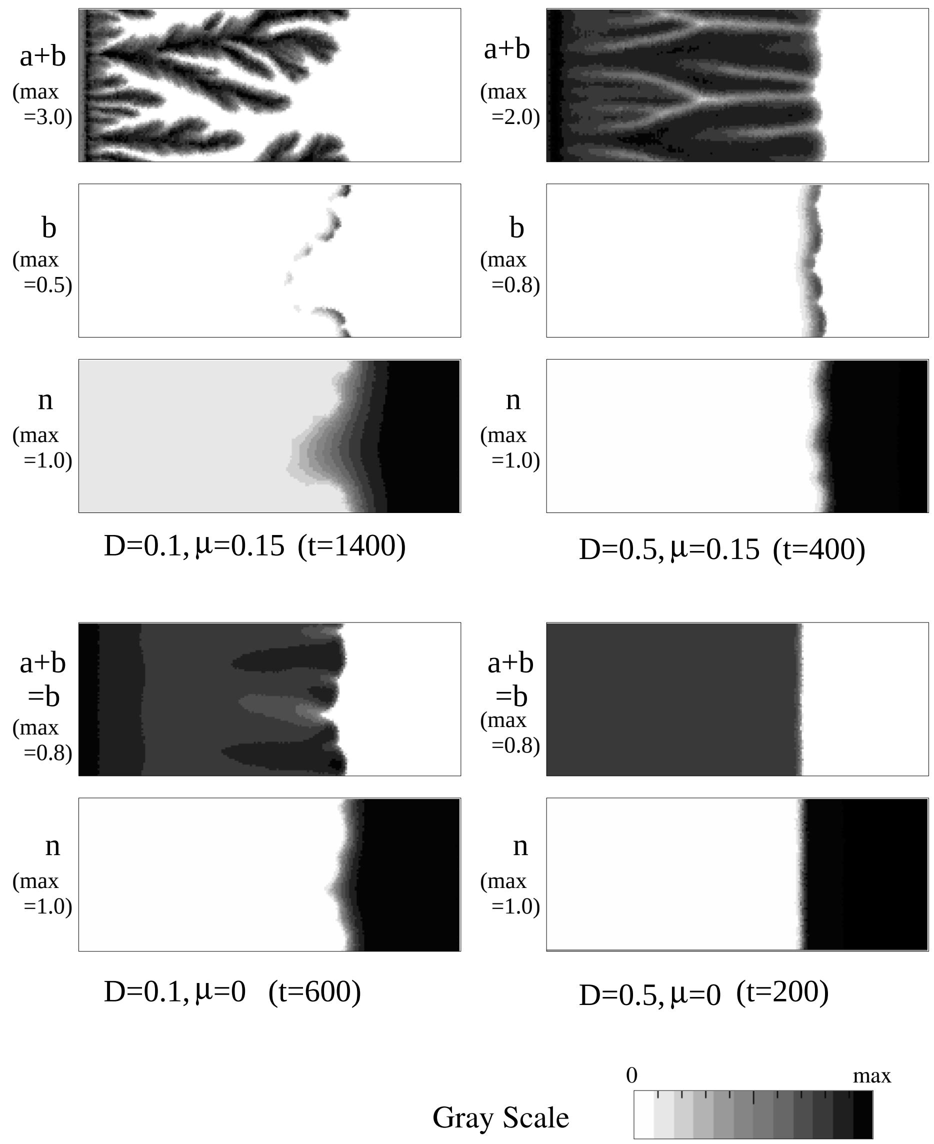

Fig. 3. For $k = 1$ and some values of D and μ, the snapshots of $a + b$, b and n are illustrated with the gray scale printed bellow. b is the same as $a + b$ for $\mu = 0$ because $a = 0$.

tiplicative constant. We presume from the discussion in §2 that vanishing k and large diffusion constant D correspond to soft agar condition, i.e., C_a small, while non-vanishing k and small D correspond to large-C_a condition. Because in experiments the bacteria are inoculated initially as a point, the colony spreads out in a circle. We observe a simple disk for large initial nutrient n_0 and small agar concentration C_a, Eden-like patterns for large n_0 and large C_a, and fingering patterns such as DLA for small n_0 and large C_a. Ring patterns do not appear in our model, and this point will be discussed in §5.

§4. Interface Dynamics

In this section, we reduce our differential equations to an interface dynamics to understand the results of the previous section more theoretically. We use a perturbation method similar to the one applied by Caginalp[13] to the phase field model[14,15] for crystal growth.

By introducing a small parameter ϵ which will turn out later to represent the width of the interface, we rewrite our equations into

$$\epsilon^2 \partial_t n = \epsilon^2 \triangle n - nb \tag{4.1a}$$

and

$$\epsilon^2 \partial_t b = \epsilon^3 D \triangle (b^{k+1}) + (n - \epsilon\mu) b. \tag{4.1b}$$

We expand these equations in ϵ like

$$n = \sum_{m=0}^{\infty} \epsilon^m n^{(m)}(x, y, t), \tag{4.2}$$

$$O(1) \quad n^{(0)}b^{(0)} = 0,$$

$$O(\epsilon) \quad n^{(1)}b^{(0)} + n^{(0)}b^{(1)} = 0, \quad \mu b^{(0)} = 0,$$

$$O(\epsilon^2) \quad \partial_t n^{(0)} = \triangle n^{(0)} - n^{(0)}b^{(2)} - n^{(1)}b^{(1)} - n^{(2)}b^{(0)}, \quad \partial_t b^{(0)} = n^{(0)}b^{(2)} + (n^{(1)} - \mu)b^{(1)} + n^{(2)}b^{(0)}.$$

These expansions are correct outside the interface because the spatial derivative ∇ is of the order of $1/\epsilon$ within the interface. Such expansions are called the outer expansions. We get the following results.

$$\text{If } n^0 \neq 0,\ \partial_t n^{(0)} = \triangle n^{(0)} \text{ and } b^{(0)} = 0. \tag{4.3a}$$

$$\text{If } n^0 = 0, \quad \begin{array}{ll} b^{(0)} = 0 & \text{for } \mu = 0. \\ \partial_t b^{(0)} = 0 & \text{for } \mu \neq 0. \end{array} \tag{4.3b}$$

Equation (4.3a) is satisfied outside the bacterial colony and, as shown later, eq.(4.3b) holds inside the colony.

In order to determine the velocity V of the interface, we next consider the inner expansions by transforming the coordinates (x, y, t) to (ξ, y, t), where $\epsilon\xi \equiv x - \phi(y, t)$ and $x = \phi(y, t)$ represents the interface perpendicular to the x-axis. Equations (4.1a) and (4.1b) now take the forms

$$\epsilon^2 \partial_t n = \partial_{\xi\xi} n + \epsilon(V + \kappa)\partial_\xi n + \epsilon^2 \partial_{yy} n - nb \tag{4.4a}$$

and

$$\epsilon^2 \partial_t b = \epsilon D(\partial_{\xi\xi} + \epsilon\kappa\partial_\xi + \epsilon^2 \partial_{yy}) b^{k+1} + \epsilon V \partial_\xi b + (n - \epsilon\mu) b \tag{4.4b}$$

on the ξ-axis, where $V \equiv \partial_t \phi$ and $\kappa \equiv -\partial_{yy}\phi$ represent the velocity and curvature of the interface, respectively. We expand them again in the form

$$n = \sum_{m=0}^{\infty} \epsilon^m \tilde{n}^{(m)}(\xi, y, t), \tag{4.5}$$

where the functions in the inner expansions are indicated with a tilde.

The boundary conditions for $\tilde{n}^{(m)}$ and $\tilde{b}^{(m)}$ are obtained from the matching conditions between the outer expansion eq.(4.2) and the inner expansion eq.(4.5). The formal ϵ-expansion

$$\sum_{m=0}^{\infty} \epsilon^m \tilde{n}^{(m)}(\xi, y, t) = \sum_{m=0}^{\infty} \epsilon^m n^{(m)}(\phi + \epsilon\xi, y, t)$$

gives the following conditions for $\tilde{n}^{(m)}$ and $n^{(m)}$ in the limit $\epsilon\xi \to 0$ and $\xi \to \infty$:

$$O(1) \quad \partial_\xi \tilde{n}^{(0)}(\pm\infty, y, t) = 0, \quad \tilde{n}^{(0)}(\pm\infty, y, t) = n^{(0)}(\phi \pm 0, y, t),$$

$$O(\epsilon) \quad \partial_\xi \tilde{n}^{(1)}(\pm\infty, y, t) = \partial_x n^{(0)}(\phi \pm 0, y, t),$$

where $\tilde{A}(\pm\infty) = A(\phi \pm 0)$ represents

$$\lim_{\xi\to+\infty} \tilde{A}(\xi) = \lim_{\delta\to 0, \delta>0} A(\phi + \delta)$$
and
$$\lim_{\xi\to-\infty} \tilde{A}(\xi) = \lim_{\delta\to 0, \delta<0} A(\phi + \delta).$$

The $O(1)$ equations for eqs.(4.4a) and (4.4b) are

$$\partial_{\xi\xi} \tilde{n}^{(0)} = \tilde{n}^{(0)}\tilde{b}^{(0)} = 0 \tag{4.6}$$

with the boundary conditions $\partial_\xi \tilde{n}^{(0)}(\pm\infty, y, t) = 0$. The only possible solution is $\tilde{n}^{(0)} = constant$, which gives the condition for continuity $n^{(0)}(\phi+0, y, t) = n^{(0)}(\phi-0, y, t)$ at the interface because $\tilde{n}^{(0)}(\pm\infty, y, t) = n^{(0)}(\phi\pm 0, y, t)$.

By substituting the solution into eqs.(4.4a) and (4.4b), the $O(\epsilon)$ equations are given as

$$\partial_{\xi\xi} \tilde{n}^{(1)} - \tilde{n}^{(1)}\tilde{b}^{(0)} - \tilde{n}^{(0)}\tilde{b}^{(1)} = 0 \tag{4.7a}$$

and

$$D\partial_{\xi\xi} \tilde{b}^{(0)k+1} + V\partial_\xi \tilde{b}^{(0)} + (\tilde{n}^{(1)} - \mu)\tilde{b}^{(0)} + \tilde{n}^{(0)}\tilde{b}^{(1)} = 0, \tag{4.7b}$$

where the boundary conditions are $\partial_\xi \tilde{n}^{(1)}(\pm\infty, y, t) = \partial_x n^{(0)}(\phi \pm 0, y, t)$ and $\partial_\xi \tilde{b}^{(0)}(\pm\infty, y, t) = 0$. We easily get $\tilde{n}^{(0)}\tilde{b}^{(1)} = 0$ from eqs.(4.6) and (4.7). Therefore, $\tilde{n}^{(1)}$ and $\tilde{b}^{(0)}$ are found by solving eq.(4.7).

We know from eq.(4.3a) and the matching conditions $\tilde{b}^{(0)}(\pm\infty, y, t) = b^{(0)}(\phi \pm 0, y, t)$ that $\tilde{b}^{(0)}(+\infty, y, t)$ is identical to zero. Because $n^{(0)}(\phi, y, t) = \tilde{n}^{(0)} = 0$ if $\tilde{b}^{(0)} \neq 0$, eq.(4.3b) is satisfied inside the colony so that $\partial_\xi \tilde{n}^{(1)}(-\infty, y, t) = 0$. If the solution of the boundary value problem eq.(4.7) is solved uniquely and turned out stable, this gives the relation between the interface velocity V and the nutrient gradient $\partial_x n^{(0)}(\phi + 0, y, t)$ at the interface.

Equations (4.7a) and (4.7b) reduce to the equations with the single parameter μ,

$$\partial_{\xi\xi} \tilde{n}^{(1)} = \tilde{n}^{(1)}\tilde{b}^{(0)} \tag{4.8a}$$

and

$$\partial_{\xi\xi} \tilde{b}^{(0)k+1} + \partial_\xi \tilde{b}^{(0)} + (\tilde{n}^{(1)} - \mu)\tilde{b}^{(0)} = 0. \tag{4.8b}$$

Here we have made rescaling $\tilde{b}^{(0)} \to B\tilde{b}^{(0)}$, $\tilde{n}^{(0)} \to N\tilde{n}^{(0)}$, $\xi \to X\xi$ and $\mu \to N\mu$, where $X \equiv (D/V)^{1/(2k+1)}$, $N \equiv V/X$ and $B \equiv 1/X^2$. When k is nonzero, we may take the origin of ξ as $\tilde{b}^{(0)}(\xi) \neq 0$ for negative ξ and as $\tilde{b}^{(0)}(\xi) = 0$ for positive ξ. Because eq.(4.8b) provides the asymptotic solution for $\tilde{b}^{(0)}$ for negative ξ, i.e.,

$$\tilde{b}^{(0)}(\xi) \to \left(-\tfrac{k}{k+1}\xi\right)^{\frac{1}{k}} \quad \text{as } \xi \to 0, \tag{4.9}$$

the nonlinearity of the equation gives the additional boundary condition

$$\partial_\xi \tilde{b}^{(0)}(0-, y, t)^k = -\frac{k}{k+1}. \tag{4.10}$$

The solution of eq.(4.8) satisfying this condition gives the relation between $\partial_x n^{(0)}(\phi + 0, y, t)$ and μ:

$$\partial_x n^{(0)}(\phi + 0, y, t) = F(\mu), \tag{4.11}$$

where we have assumed the solution stable.

With the original scale, this relation describes the magnitude of the nutrient gradient $|\nabla n^{(0)}| \equiv \partial_x n^{(0)}(\phi + 0, y, t)$ at the interface as a function of the velocity V as follows,

$$|\nabla n^{(0)}| = V\left(\frac{V}{D}\right)^{\frac{2}{2k+1}} F\left(\frac{\mu}{D}\left(\frac{D}{V}\right)^{\frac{2k+2}{2k+1}}\right). \tag{4.12a}$$

Supplemented with the equations

$$\begin{cases} \partial_t n^{(0)} = \triangle n^{(0)} & \text{outside the colony} \\ n^{(0)} = 0 & \text{inside the colony,} \end{cases} \quad (4.12b)$$

the interface dynamics is thus completed. We note that the interface dynamics can not be constructed for vanishing k because the additional boundary condition (4.10) is given by the nonlinearity of eq.(4.8b).

We computed $F(\mu)$ in eq.(4.11) by solving the boundary value problem eqs.(4.8) and (4.10) with the relaxation method. Figure 4 shows $F(\mu)$ for some values of k. We summarize the feature of $F(\mu)$.

1. $F(0)$ is nonzero and increases with k. Therefore, for vanishing μ or for large V,

$$|\nabla n^{(0)}| \propto V \left(\frac{V}{D}\right)^{\frac{2}{2k+1}}. \quad (4.13)$$

2. $F(\mu) \propto \mu^{\alpha(k)}$ for large μ, where $\alpha(k)$ is an increasing function for k and $\alpha(1) \simeq 0.5$ as shown in Fig.5. The functional form for large μ describes the movement of the interface for small V, because

$$|\nabla n^{(0)}| \propto V^{\zeta} \quad \text{as } V \to 0, \quad (4.14)$$

where $\zeta = [2k+3-(2k+2)\alpha]/(2k+1)$. In particular, $|\nabla n^{(0)}|$ is proportional to V when $\alpha = 0.5$, or $k \simeq 1$.

3. $F(\mu) \to 0$ for the limit $k \to 0$.

In the next section, we will discuss the patterns obtained in §3 on the basis of these results.

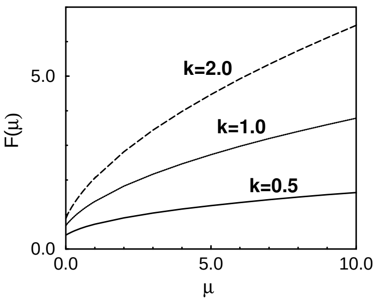

Fig. 4. $F(\mu)$ are calculated for $k = 0.5$,1.0 and 2.0.

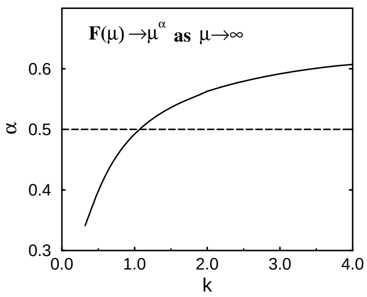

Fig. 5. The power $\alpha(k)$ of $F(\mu)$ for large μ.

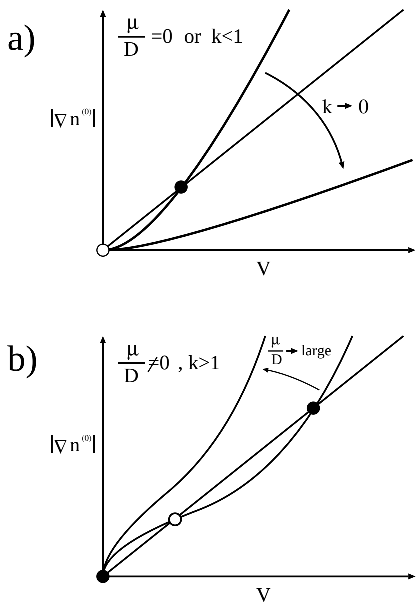

Fig. 6. $|\nabla n^{(0)}|$ are illustrated as functions of V, when $\mu/D = 0$ or $k < 1$ in a) and when $\mu/D \neq 0$ and $k > 1$ in b).

§5. Discussions

For non-vanishing k, we constructed the interface dynamics eq.(4.12). We first consider the interface in one-dimensional space x. Because the steadily propagating solution of eq.(4.12b) is given by

$$n^{(0)} = \begin{cases} 1 - e^{-V(x-Vt)} & x \geq Vt \\ 0 & x < Vt, \end{cases} \quad (5.1)$$

the nutrient gradient $|\nabla n^{(0)}|$ at the interface approaches V if the velocity V is fixed. By inspection of the fixed points $|\nabla n^{(0)}| = V$, we notice that eq.(4.12a) has three types of the behavior as illustrated in Fig.6.

i) For vanishing μ/D or $k < 1$, there are an unstable fixed point at $V = 0$ and a stable one at finite V to which the velocity of the interface always tends.
ii) When μ/D is finite and small for $k > 1$, bistability appears with two stable fixed points at $V = 0$ and finite V.
iii) When μ/D is large for $k > 1$, there is only one stable point at $V = 0$. Consequently, the steadily propagating solution does not exist in one-dimensional space.

We note that the stability of the state $V = 0$ is a result of combined effects of the nonlinear diffusion and the suspension of the activity.

In two-dimensional space, change in the stability of the state $V = 0$ is expected to change the movement of the interface in the poor nutrient concentration. Although a straight interface propagating with a constant speed is always unstable as shown in Appendix, we saw already by the numerical simulations in §3 that fingers do not grow in the parameter region i), but they do in ii) and iii).

The fingers develop stronger with increasing μ/D. When the velocity V is so small that the system size is much larger than D_n/V, eq.(4.12b) may be approximated by Laplace equation; $\triangle n^{(0)} = 0$. Because eq.(4.14) approximates $|\nabla n^{(0)}|$, this is nothing but a standard model[16,17] generating fractal patterns. It should be noted, however, that the surface tension does not work in the dynamics because the curvature κ contributes to $|\nabla n^{(0)}|$ in eq.(4.11) only to the order of ϵ. In that case, the interface dynamics breaks down due to the development of cusps. Therefore, developed fingers are expected to have a characteristic width of the order of ϵ, i.e., the thickness of the interface. This point makes a difference from the normal viscous fingering where the surface tension effect plays an important role in determining the shape of a finger.

Finally, we consider the case of normal diffusion $k = 0$. We know from the asymptotic form of eq.(4.9) that, as k decreases to zero, the origin of ξ in §4, where the bacterial density $b(\xi)$ vanishes, does not coincide with the natural front where $b(\xi)$ decreases most rapidly. Consequently, the front propagation for vanishing k is not described as the limit of vanishing k in the interface dynamics discussed above. When k equals zero, our model gives a kind of Fisher-type equations, whose velocity selection for the propagating front has been studied by many people[18-23]. "The linear marginal hypothesis" proposed by W. van Saarloos[24] gives the asymptotic speed $V = 2\sqrt{D(1-\mu)}$ of the propagating front for eq.(2.3) and this agrees with the results of our numerical simulations. We also observed numerically in §2 that the straight front is always stable. How the normal diffusion changes into the nonlinear one and what happens then will be a future problem. Experimentally, ring and DBM patterns appear in the corresponding parameter region.

§6. Conclusions

We proposed the differential-equation model for the pattern formation of the bacterial colonies, and carried out its numerical simulations. Our results are consistent with experiments. Our model was reduced to an interface dynamics by using a systematic perturbation expansion. It is similar to a system exhibiting normal viscous fingering except that it does not include a surface tension effect. We discussed that the appearance of fingering patterns requires both the effects of nonlinear diffusion and suspension of the activity of the bacteria. The difference between the normal and the nonlinear diffusion is also considered in the framework of the interface dynamics.

Acknowledgment

The author acknowledges Y. Kuramoto, T. Mizuguchi and other members of Nonlinear Dynamics group in Kyoto University. The author is grateful to M. Matsushita, A. Nakahara and J. Wakita for fruitful discussions about their experiments and to S. Sasa for some valuable suggestions.

Appendix: Linear Stability Analysis of eq.(4.12) for a straight interface

We include surface tension effect into eq.(4.12) and consider the equation

$$\partial_t n = \triangle n \tag{A·1a}$$

with the conditions

$$\begin{cases} n = 0 \\ V = G(|\nabla n|) - \gamma\kappa \end{cases} \quad \text{at the interface,} \tag{A·1b}$$

where κ represents curvature of the interface and γ is a constant. The steadily propagating solution with velocity V_s is described as

$$n = 1 - e^{-V_s(x - V_s t)} \quad \text{for } x \geq V_s t, \tag{A·2}$$

where $V_s = G(V_s)$ and $x = V_s t$ represents the position of the interface. We investigate linear stability of this solution.

We set $V_s = 1$ without loss of generality because this is always possible by the scaling $V_s\mathbf{x} \to \mathbf{x}$ and $V_s^2 t \to t$. By making a transformation into the moving coordinates; $x - \phi(y,t) \to x$, eq.(A·1) becomes

$$\partial_t n = \{[1+(\partial_y\phi)^2]\partial_{xx} + \partial_{yy} + (\partial_t\phi - \partial_{yy}\phi)\partial_x - 2\partial_y\phi\partial_{xy}\}n, \tag{A·3}$$

where $x = \phi(y,t)$ represents the interface and the steadily propagating solution eq.(A·2) is described with the equation

$$n = n_s(x) \equiv 1 - e^{-x} \quad \text{for } x \geq 0 \tag{A·4}$$

with $G(1) = 1$.

We consider small perturbations

$$\begin{cases} \phi(y,t) = t + \delta\phi_{\lambda,q} e^{\lambda t}\cos qy \\ n(x,y,t) = n_s(x) + \delta n_{\lambda,q}(x) e^{\lambda t}\cos qy. \end{cases} \tag{A·5}$$

Because V and κ represent $\partial_t\phi$ and $-\partial_{yy}\phi$, respectively, the linearized equations are given by

$$(\nu - \mathcal{L}_s)\delta n_{\lambda,q} = \nu\delta\phi_{\lambda,q}\partial_x n_s \tag{A·6a}$$

and

$$\lambda\delta\phi_{\lambda,q} = G'\partial_x\delta n_{\lambda,q}|_{x=0} - \gamma q^2\delta\phi_{\lambda,q}, \tag{A·6b}$$

where $\nu \equiv \lambda + q^2$, $\mathcal{L}_s \equiv \partial_{xx} + \partial_x$ and $G' \equiv dG(V_s)/d|\nabla n|$.

The translational mode is a particular solution of eq. (A·6a), $\mathcal{L}_s\partial_x n_s = 0$. Therefore, the general solutions are given in the form

$$\delta n_{\lambda,q}(x) = \delta\phi_{\lambda,q}\partial_x n_s(x) + u_\nu(x), \tag{A·7}$$

where $u_\nu(x)$ satisfies $(\nu - \mathcal{L}_s)u_\nu = 0$. The boundary conditions $u_\nu(0) = -\delta\phi_{\lambda,q}$ and $u_\nu(\infty) = 0$ are imposed on $u_\nu(x)$ because $\delta n_{\lambda,q}(0) = \delta n_{\lambda,q}(\infty) = 0$ and $\partial_x n_s(0) = 1$. By substituting eq.(A·7) to eq.(A·6b), λ is found in the form

$$\lambda = -G'(1 + \partial_x \log u_\nu|_{x=0}) - \gamma q^2 \tag{A·8}$$

where we used $\partial_{xx}n_s(0) = -1$.

Because $u_\nu(x)$ is proportional to $e^{-x(1+\sqrt{1+4\nu})/2}$, we obtain an analytical form for λ:

$$\lambda = \frac{G'(G'-1)}{2}\left[1 \pm \sqrt{1 + \frac{4(1-\gamma)}{(1-G')^2}q^2}\right] - \gamma q^2 \quad (\mathrm{A\cdot 9})$$

Stability of the straight interface propagating with a finite velocity depends on the value of G':

$G' < \gamma$: stable for the all modes.
$\gamma < G' < 1$: unstable for the long wave perturbations.
$1 < G'$: unstable for the translational mode.

Therefore, the straight interface propagating with constant velocity is always unstable because γ is $O(\epsilon)$ in eq.(4.12). If G is proportional to $|\nabla n|^{1/\zeta}$ as eq.(4.14), G' equals $1/\zeta$. The unstable fixed point discussed in §5 corresponds to the case $1 < G'$.

The above results are also applied to the interface with small curvature κ_s by rewriting V_s to $V_s + \kappa_s$, where $G' \equiv dG(V_s + \kappa_s)/d|\nabla n|$ and the velocity V_s is given by the equation $V_s = G(V_s + \kappa_s) - \gamma\kappa_s$. Because $G' = 1/[(1 + \kappa_s/V_s)\zeta]$ if $G \propto |\nabla n|^{1/\zeta}$, the interface generally becomes more stable with the increase of the curvature.

1) E. O. Budrene and H. C. Berg: Nature **349**(1991) 630.
2) T. Matsuyama and M. Matsushita: Critical Reviews in Microbiology **19**(1993) 117-35.
3) Y. Shimada, A. Nakahara, M. Matsushita and T. Matsuyama: J.Phys.Soc.Jpn. **64**(1995) No.6 1896-9.
4) M. Ohgiwari, M. Matsushita and T. Matsuyama: J.Phys.Soc. Jpn. **61**(1992) No.3 816-22.
5) H. Fujikawa: Physica A **189**(1992) 15-21.
6) J. Wakita, K. Komatsu, A. Nakahara, T. Matsuyama and M. Matsushita: J.Phys.Soc.Jpn. **63**(1994) No.3 1205-11.
7) E. Ben-Jacob ,O. Schochet, A. Tenenbaum, I. Cohen, A. Czirók and T. Vicsek: Nature **368**(1994) 46-9.
8) E. Ben-Jacob , O. Shodhet, A. Tenenbaum and O. Avidan: *Spatio-Temporal Patterns in Nonequilibrium Complex Systems, Proc. NATO Advanced Research Workshop*, ed. P. E. Cladis and P. Pallffy-Muboray (Addison-Wesley, 1995) p.619-33.
9) K. Kwasaki, A.Mochizuki and N.Shigesada: J.SICE (in Japanese) **34**(1995) No.10 811-816.
10) M. Mimura and H. Sakaguchi: They reported an interesting model for the ring patterns in Japan, perhaps, to be published.
11) R. Friedberg and H.-C. Ren: Nuclear Physics B **235**(1984) 310-20.
12) C. Moukarzel: Physica A **190**(1992) 13-23.
13) G. Caginalp: Phys.Rev.A **39**(1989) No.11 5887-96.
14) R. Kobayashi: Physica D **63**(1993) No.3-4 410-23.
15) G. Caginalp and P. Fife: Phys.Rev.B **33**(1986) No.11 7792-4.
16) L. Niemeyer, L. Pietronero and H.J.Wiesmann: Phys.Rev. Lett. **52**(1986) No.12 1033-6.
17) M. Matsushita, K. Honda, H. Toyoki, Y. Hayakawa and H. Kondo: J.Phys.Soc.Jpn. **55**(1986) No.8 2618-26.
18) D. G. Aronson and H. F. Weinberger: *Partial Differential Equations and Related Topics*, ed. J.A.Goldstein (Springer, New York, 1975) p.5-49.
19) G. Dee and J. S. Langer: Phys.Rev.Lett. **50**(1983) No.6 383-86.
20) G. C. Paquette and Y. Oono: Phys.Rev.E **49**(1994) No.3 2368-88.
21) G. C. Paquette, L. Chen, N. Goldenfeld and Y. Oono: Phys.Rev.Lett. **72**(1994) No.1 76-79.
22) W. van Saarloos: Phys.Rev.A **37**(1988) No.1 211-29.
23) W. van Saarloos: Phys.Rev.A **39**(1989) No.12 6367-90.
24) W. van Saarloos: Phys.Rev.Lett. **58**(1987) No.24 2571-4.